

NEWS: the near-infrared Echelle for wideband spectroscopy

Mark J. Veyette^a, Philip S. Muirhead^a, Zachary J. Hall^a, Brian Taylor^{a,b}, and Jimmy Ye^{a,c}

^aDepartment of Astronomy, Boston University, 725 Commonwealth Ave., Boston, MA, USA

^bTI Research, 2915 Kletha Trail, Flagstaff, Az, USA

^cDepartment of Physics, College of the Holy Cross, 1 College Street, Worcester, MA, USA

ABSTRACT

We present an updated optical and mechanical design of NEWS: the Near-infrared Echelle for Wide-band Spectroscopy (formerly called HiJaK: the High-resolution J, H and K spectrometer), a compact, high-resolution, near-infrared spectrometer for 5-meter class telescopes. NEWS provides a spectral resolution of 60,000 and covers the full 0.8–2.5 μm range in 5 modes. We adopt a compact, lightweight, monolithic design and developed NEWS to be mounted to the instrument cube at the Cassegrain focus of the the new 4.3-meter Discovery Channel Telescope.

Keywords: infrared astronomy, infrared spectroscopy, low-mass stars, exoplanets, stellar abundances

1. INTRODUCTION

High-resolution, near-infrared (NIR) spectroscopy enables an enormously broad range of scientific studies (see Ref. 1 and references therein). However, relatively few facility-class, high-resolution, NIR spectrometers currently exist. Most are only available on large, heavily subscribed 8-to-10 meter class telescopes, such as NIRSPEC on the 10-meter Keck II Telescope,² CRILES on the 8.2-meter VLT UT 1 Telescope,³ and IRCS on the 8.2-meter Subaru Telescope.^{4,5} High-resolution, NIR spectrometers for 3–5-meter class telescopes like Lowell Observatory’s new 4.3-meter Discovery Channel Telescope⁶ (DCT) in Happy Jack, Arizona would provide greater accessibility for this powerful yet under-utilized tool for astronomy.

Offering continuous, wide-band coverage has been an obstacle for high-resolution, NIR spectrometers. The number of resolution elements ($\Delta\lambda$) within the free spectral range (FSR) of a single order of a grating-based spectrometer is given by

$$\frac{\text{FSR}}{\Delta\lambda} = \frac{\lambda N}{\phi D}, \quad (1)$$

where λ is the wavelength at the center of the order, N is the number of illuminated grooves, ϕ is the angular width of the slit, and D is the diameter of the telescope. Traditionally, higher resolution is achieved by increasing N by using a larger grating or a grating with more closely spaced grooves. In the IR, the number of resolution elements per order quickly becomes too large to fit a full order across a single detector with at least two pixels per resolution element to fully sample the spectrum.

Immersion gratings provide one path to high resolution while maintaining small free spectral ranges. Spectral resolution increases linearly with the index of refraction of the medium the grating is immersed in. IGRINS⁷ and iSHELL⁸ both achieve high-resolution ($R > 40,000$) across the NIR through the use of a silicon ($n = 3.4$) immersion grating. However, silicon is not transmissive below 1.2 μm . At constant resolution, the 0.8 to 1.2 μm range accounts for over 35% of the information content in the 0.8 to 2.5 μm range. As we discuss in Section 2, Y-band around 1 μm is a requirement for our primary science goal.

Resolution also increases linearly with $\tan(\delta)$, the tangent of the blaze angle. With a high-blaze Echelle grating, high resolution can be achieved in a format that can be imaged by a single 2k×2k detector. Here we present an optical design for a high-resolution NIR spectrograph called NEWS: the Near-infrared Echelle for Wide-band Spectroscopy. The design is based on a high-blaze R6 ($\tan(\delta) = 6$) Echelle grating and achieves a resolution of 60,000 over the full 0.8–2.5 μm range. The photometric z, Y, J, H, and K bands can be observed in their entirety without gaps.

Send correspondence to M.J.V., e-mail: mveyette@bu.edu

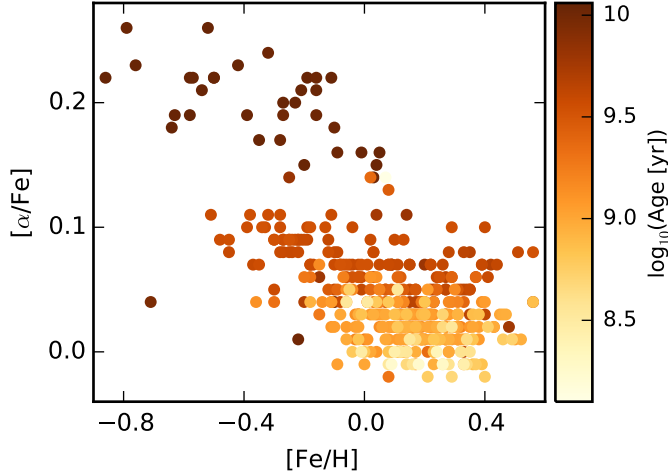


Figure 1. The $[\alpha/\text{Fe}]$ - $[\text{Fe}/\text{H}]$ -age relation based on nearby red giants (data from Ref. 23). This relation can provide ages for field M dwarfs given a method to measure $[\alpha/\text{Fe}]$ in M dwarfs.

2. SCIENTIFIC MOTIVATION

The primary science goal of NEWS is to measure the abundances of individual elements in M dwarf stars. One application of this capability is to measure the ages of field M dwarfs. M dwarf stars are the most common class of star in the Galaxy, accounting for 70% of all stars.⁹ Their small radii and low effective temperatures ($2500\text{K} < T_{\text{eff}} < 3800\text{K}$) make nearby M dwarfs well suited for the detection of small, potentially habitable planets. Results from NASA’s *Kepler* Mission suggest M dwarfs are teeming with planets with ~ 1 rocky planet per M dwarf with a period < 150 days.^{10,11} NASA’s *Transiting Exoplanet Survey Satellite* (*TESS*) is expected to discover over 400 Earth-sized planets around nearby M dwarfs, including ~ 50 orbiting within their host stars’ habitable zones.¹²

M dwarfs’ low effective temperatures make them difficult to characterize due to the formation of molecules throughout their atmospheres. Their visible and NIR spectra are dominated by millions of molecular lines that blend together even at high resolution. These molecular features render useless the standard methods developed for inferring fundamental parameters like T_{eff} , surface gravity, and chemical composition of Sun-like stars.

The age of an M dwarf is perhaps the most challenging fundamental parameter to measure but enables a wide variety of stellar and exoplanet science. M dwarfs are known to host a wide range of planetary architectures: single short-period gaseous planets (e.g. GJ 1214 b¹³), compact multiple systems (e.g. *Kepler*-42, *Kepler*-445, and *Kepler*-446^{14,15}), single rocky planets, and multi-planet systems with a wide range of planet masses. Ages of the host M dwarfs in these systems would answer outstanding questions on planet formation and evolution. It is an open question whether the scarcity of short-period gaseous planets is due to lower disk surface density around M dwarfs¹⁶ or if they are a short-lived evolutionary state, evaporated by high UV flux.¹⁷ Theorists disagree on the timescales for orbital evolution of short-period planets orbiting M dwarfs. Ref. 18 argue the tidally-induced eccentricity-damping timescale for short-period, low-mass planets is small, such that they should be circularized by 1 Gyr. However, Ref. 19 argue that eccentricity-damping is coupled to semi-major axis damping, extending the timescale to many billions of years. These competing hypotheses are testable given a means to measure M dwarf ages.

Unlike solar-type stars, main-sequence M dwarfs move imperceptibly on a color-magnitude diagram. Gyrochronology, or the study of stellar spin-down versus age, holds some promise for measuring M dwarf ages. However, recent studies of M dwarfs with age-dated white dwarf companions suggest that M dwarfs do not spin down efficiently,²⁰ and can hold onto their rapid rotation for billions of years.^{21,22}

Our knowledge of the chemical evolution of the Galaxy provides a novel tool for estimating the ages of field M dwarfs. Early in the life of the Galaxy, core-collapse supernovae enrich the interstellar medium with the

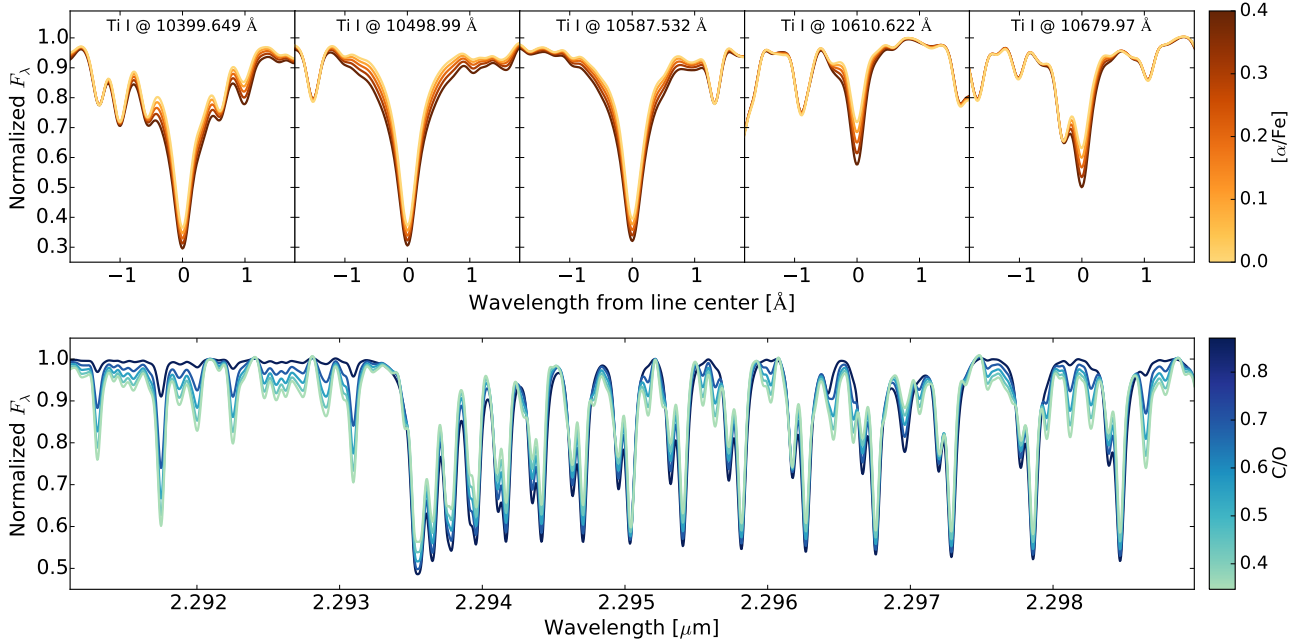


Figure 2. Pseudo-continuum normalized synthetic M dwarf spectra ($T_{\text{eff}}=3000$ K, $\log(g)=5.0$, $[M/H]=0.0$) smoothed to $R = 60,000$. Top: A representative sample of deep, $[\alpha/\text{Fe}]$ -sensitive ^{48}Ti I lines in Y-band for models with varied $[\alpha/\text{Fe}]$. Bottom: K-band metal lines and the CO 2-0 bandhead for models with varied C/O. High-resolution Y-band and K-band observations can be used to measure α -abundance in M dwarf stars and calibrate out any effects of C and O abundance.

α -elements O, Ne, Mg, Si, S, Ca, and Ti. Subsequently, type Ia supernovae contribute large amounts of Fe and the relative abundance of α -elements to Fe ($[\alpha/\text{Fe}]$) decreases. Surveys of nearby Sun-like stars and red giants find an empirical relation between $[\alpha/\text{Fe}]$, $[\text{Fe}/\text{H}]$, and age.^{23–25} Figure 1 shows the $[\alpha/\text{Fe}]$ - $[\text{Fe}/\text{H}]$ -age relation for nearby red giants. We determined $[\alpha/\text{Fe}]$ and $[\text{Fe}/\text{H}]$ can be used to measure ages to an accuracy of ± 1 Gyr root-mean-square. This relation provides a new, powerful tool for estimating ages of field M dwarfs, given methods to measure their $[\alpha/\text{Fe}]$ and $[\text{Fe}/\text{H}]$. The correlation between $[\alpha/\text{Fe}]$, $[\text{Fe}/\text{H}]$, and age is not perfect given the chaotic nature of star formation and availability of pristine gas even in the late stages of galaxy evolution. Ref. 26 found that 6% of nearby red giants with $[\alpha/\text{Fe}] > 0.13$ are younger than 6 Gyr. Nevertheless, measurements of $[\alpha/\text{Fe}]$ and $[\text{Fe}/\text{H}]$ can be combined into a powerful statistical tool for estimating ages of field M dwarfs.

Recently multiple methods for measuring metallicity of M dwarfs have been empirically calibrated via widely-separated binary systems composed of an M dwarf with an FGK companion. The two stars are assumed to have formed at the same time, from the same material and, therefore, share a common chemical composition. Metal-sensitive indicators in M dwarf spectra can be calibrated on metallicities measured from the FGK companion. Methods have been developed to measure M dwarf metallicity from high-resolution NIR spectra,^{27,28} high-resolution optical spectra,^{29–31} moderate-resolution NIR spectra,^{32–36} and optical-NIR photometry.^{37–43}

Precise methods for measuring both $[\alpha/\text{Fe}]$ and $[\text{Fe}/\text{H}]$ are needed to estimate ages of field M dwarfs. Currently, no method exists to measure α -enhancement. Based on PHOENIX BT-Settl synthetic spectra, we found that Y-band around $1 \mu\text{m}$ contains numerous α -sensitive lines including many deep ^{48}Ti I lines. ^{48}Ti is a rapid decay product of ^{48}Cr , a product of the α process during core collapse supernovae. Figure 2 shows synthetic spectra of M dwarfs with varied abundance of the major α tracers Mg, Si, and Ti. Y-band contains numerous isolated ^{48}Ti I lines whose strength correlate with $[\alpha/\text{Fe}]$. However, these atomic lines are embedded within molecular absorption bands of TiO and FeH. High spectral resolution is required to sufficiently isolate atomic ^{48}Ti lines to measure $[\alpha/\text{Fe}]$ in M dwarfs.

It has recently been discovered that the relative abundances of carbon and oxygen strongly affect the pseudo-continuum level throughout M dwarf spectra.⁴⁴ In order to accurately measure $[\alpha/\text{Fe}]$ in M dwarfs, we must

first calibrate out any effect of C and O abundances (or their ratio* C/O) on the equivalent widths (EWs) of ^{48}Ti I lines in Y-band. Ref. 45–47 found that high-resolution observations of H_2O and CO lines in K-band can be used measure C and O abundances in M dwarfs. Figure 2 shows synthetic spectra of M dwarfs with varied C/O. In the atmosphere of an M dwarf, nearly all the C is locked away in energetically favorable CO, along with an equal amount of O. At $T_{\text{eff}} < 3300$ K, the majority of the remaining O is found in H_2O . The strength of the $2.3\text{ }\mu\text{m}$ CO 2-0 bandhead and the $1.9\text{ }\mu\text{m}$ H_2O band can be used to measure C/O.

The science case above led us to the following design requirements. NEWS must achieve high-resolution ($R > 30,000$) and cover a large portion of the NIR window, from Y-band to K-band. We find that a resolution of $R = 60,000$ provides a good balance between isolating atomic lines in M dwarf spectra but still allowing broadband observations in a single exposure. The design must also offer high throughput ($> 10\%$) in order to achieve high enough signal-to-noise to measure small changes in the EWs of atomic lines in M dwarf spectra. This requirement led us to use a slit-fed design mounted directly to the telescope as opposed to a bench-mounted, fiber-fed design which can be limited by modal noise (e.g. GIANO⁴⁸). Although the ability to measure individual elemental abundances and ages of M dwarfs has dictated many of the design requirements for NEWS, we adopted an overall facility-class philosophy. Specifically, we designed NEWS to cover the full $0.8\text{--}2.5\text{ }\mu\text{m}$ range without gaps and offer multiple slit widths and lengths. We also developed NEWS to be extremely compact and lightweight so that the design can be implemented at nearly any 3–5 meter class telescope.

3. OPTICAL DESIGN

3.1 From Telescope to Detector

We show the full NEWS optical layout in Figure 3 and list the key properties of the design in Table 1. The converging $f/6.1$ beam delivered from the telescope enters the cryostat through a fused silica window. The beam comes to a focus at one of six slits accessible by a slit wheel before passing through one of five order-selecting filters accessible by a filter wheel. The beam is then folded onto an Offner relay that serves as a cold pupil stop. After exiting the Offner relay, the beam goes through a second focus and expands to a diameter of 4 cm before being collimated by a parabolic mirror used off-axis. The collimated beam is reflected by an R6 Echelle grating that is tilted from Littrow by an in-plane angle of $\theta = 2^\circ$ and by an off-plane angle of $\gamma = 1.5^\circ$. The dispersed beam is refocused by the same parabolic mirror and is folded by a Mangin mirror to remove aberrations introduced by dispersing onto the parabolic mirror and direct the beam to the conjugate point of the same parabolic mirror. The re-collimated beam is cross-dispersed by a grating before being focused by an 8-element, all-spherical camera onto a Hawaii 2-RG detector.

3.1.1 Slit Selection

The NEWS design equips a motorized wheel to cycle through six different slit options. The width options for the slits are either $0''.5$, $1''.0$, or $1''.5$ in the dispersion direction to enable observations during nights with poor seeing at reduced resolution. The slits are either $5''$ or $9''$ long. In order to fully separate adjacent orders, only the $5''$ slit can be used with the 6th and 7th orders of the cross-disperser (corresponding to z- and Y-band). Slits will be laser-cut into 2-inch diameter gold-coated silicon wafers. Tilted slit substrates direct a $\sim 6\text{ arcmin}^2$ field back out of the cryostat where a slit-viewing camera images it onto an InGaAs detector.

3.1.2 Collimation

A monolithic parabolic mirror collimates the beam for both the Echelle and cross-disperser. The NEWS design employs a Mangin mirror to remove aberrations introduced by dispersing onto the parabolic mirror and to steer the beam returned by the Echelle to the conjugate point of the paraboloid for collimation onto the cross-disperser. The Mangin reflector is a spherical CaF_2 lens with curvature on both sides and a reflective coating on one side.

*C/O is defined as $N_{\text{C}}/N_{\text{O}}$, where N_{C} and N_{O} are the number densities of carbon and oxygen, respectively.

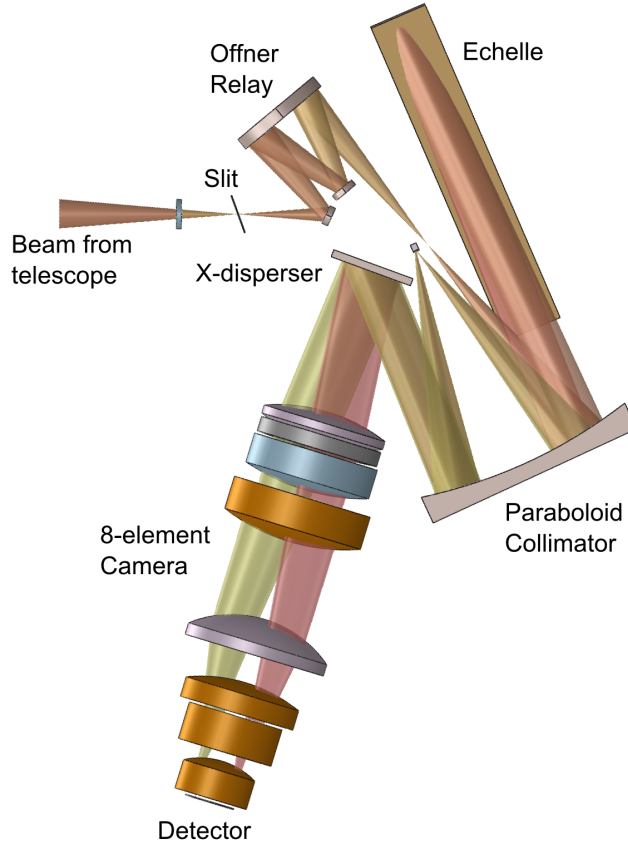


Figure 3. CAD rendering of the NEWS optical layout.

3.1.3 Primary Dispersion

We designed NEWS around a new R6 Echelle recently developed by Richardson Gratings with a coarse groove spacing and high blaze angle (13.3 grooves/mm, blazed at 80.5°). The high blaze angle and coarse grooves enable high spectral resolution with a manageable number of resolution elements per order so that the entire echellogram can be imaged by a single square detector with sufficient sampling. The Echelle is tilted in-plane by $\theta = 2^\circ$ in order to return the full $0.8\text{--}2.5\ \mu\text{m}$ range without gaps. The in-plane tilt reduces the peak efficiency by $\sim 30\%$. The Echelle is also tilted off-plane by $\gamma = 1.5^\circ$ to separate the incoming and outgoing beams at the intermediate focus.

3.1.4 Cross Dispersion

For cross-dispersion, we utilize the same grating that is used as the primary dispersive grating in TripleSpec⁴⁹ and GNIRS.⁵⁰ The grating has 110.5 grooves/mm and is blazed at 22° . Orders 7, 6, 5, 4, and 3 of the cross-disperser correspond roughly to the z, Y, J, H, and K atmospheric windows, respectively. Only a single cross-dispersion order is accessible at a time and is selected by order-blocking filters.

3.1.5 Spectrograph Camera

We designed an 8-element, all-spherical $f/2.6$ camera to image the spectrum onto a $2k \times 2k$ Teledyne Hawaii 2-RG detector with a $2.5\ \mu\text{m}$ cutoff. The camera consists of two CaF_2 , one Infrasil, one Fused Silica, and 4 ZnSe lenses. Figure 4 shows the optical layout of the camera.

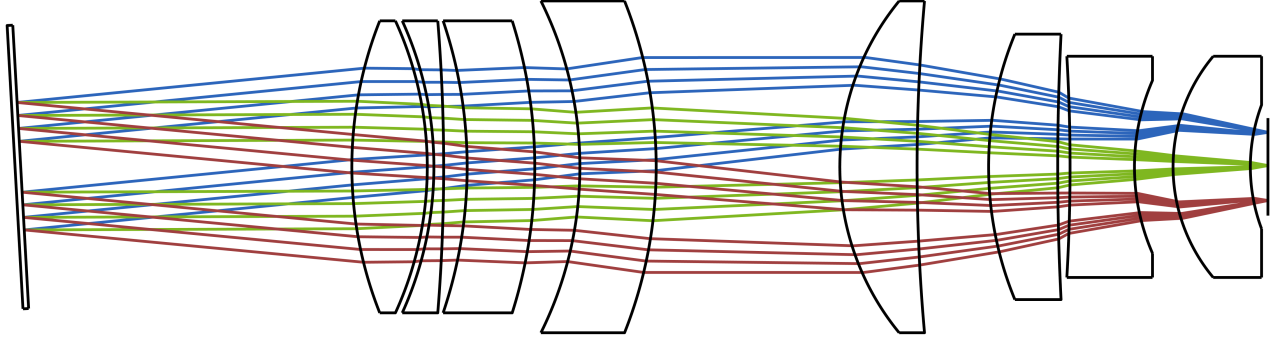


Figure 4. Camera Optical layout.

NEWS Fundamental Properties	
Resolution ($\lambda/\Delta\lambda$)	60,000 for 0".5 slit width, 30,000 for 1".0 slit width
Wavelength coverage	5 bands: Either 0.80-1.0 (<i>z</i>), 1.00-1.20 (<i>Y</i>), 1.20-1.45 (<i>J</i>), 1.45-1.85 (<i>H</i>) or 1.85-2.5 μm (<i>K</i>), selectable by filter wheel
Slit sizes on sky	6 unique sizes: either 0".5, 1".0 or 1".5 wide (dispersion directions), and either 9".0 or 5".0 long, laser cut into Au-coated Si substrates, selectable by slit wheel. Optimal slit length choice depends on band due to x-dispersion. One substrate lacks a slit for acquiring cold darks.
Beam size on Echelle	1.57 inches (4 cm)
End-to-end throughput	5% requirement, 10% goal
DCT Properties	4.3-meter diameter, Alt/az, RitcheyChretien, f/6.1 at Cassegrain, 127 μm per arcsecond
Field Rotation	Instrument mount rotation built into DCT Cassegrain cube ⁵¹
Atm. Disp. Correction	None (slit can be rotated to parallactic angle via the Cassegrain cube)
Slit Viewer Camera	COTS InGaAs detector and short-wave infrared (SWIR) lens system external to cryostat operated in <i>J</i> band (similar to NIHTS ⁵²)
Guiding	Native DCT Off-axis guider
Cold stop	Offner relay (identical to NIHTS ⁵²)
Echelle	Newport/Richardson 53-*-182E operated in quasi-Littrow (13.33 l/mm, 80.54°Blaze)
Cross-disperser	Newport/Richardson 53-*-138R operated with in-plane tilt (110.5 l/mm, 22°Blaze, identical to TSPEC ⁴⁹ and GNIRS ⁵⁰)
Spec. Camera	8-element, all spherical, f/2.6, CaF ₂ , ZnSe, Infrasil, and fused silica lenses
Spec. Detector	2.5- μm -cutoff Teledyne Hawaii-2RG (2048x2048 18- μm pixels)
Spec. Detector Electronics	Teledyne SIDECAR or Leach and custom detector interface board
Sampling	2.0 pixels per 0".5 resolution element (at R=60,000)
Cryostat	Box-style, aluminium (e.g. Atlas Ultrahigh Vacuum)
Optical Bench	39 × 25 × 12 in (99 × 64 × 30 cm) custom honey-combed aluminum
Optical Bench Temperature	Less than 100 Kelvin via a CTI-1050 cryodyne refrigeration system, 65 W max load, similar design to Mimir ⁵³
Detector Temperature	Less than 78 Kelvin via a CTI-1050 cryodyne refrigeration system, similar design to Mimir ⁵³
Total weight	<200 kg, within limit for the Cassegrain cube

Table 1. News Fundamental Parameters

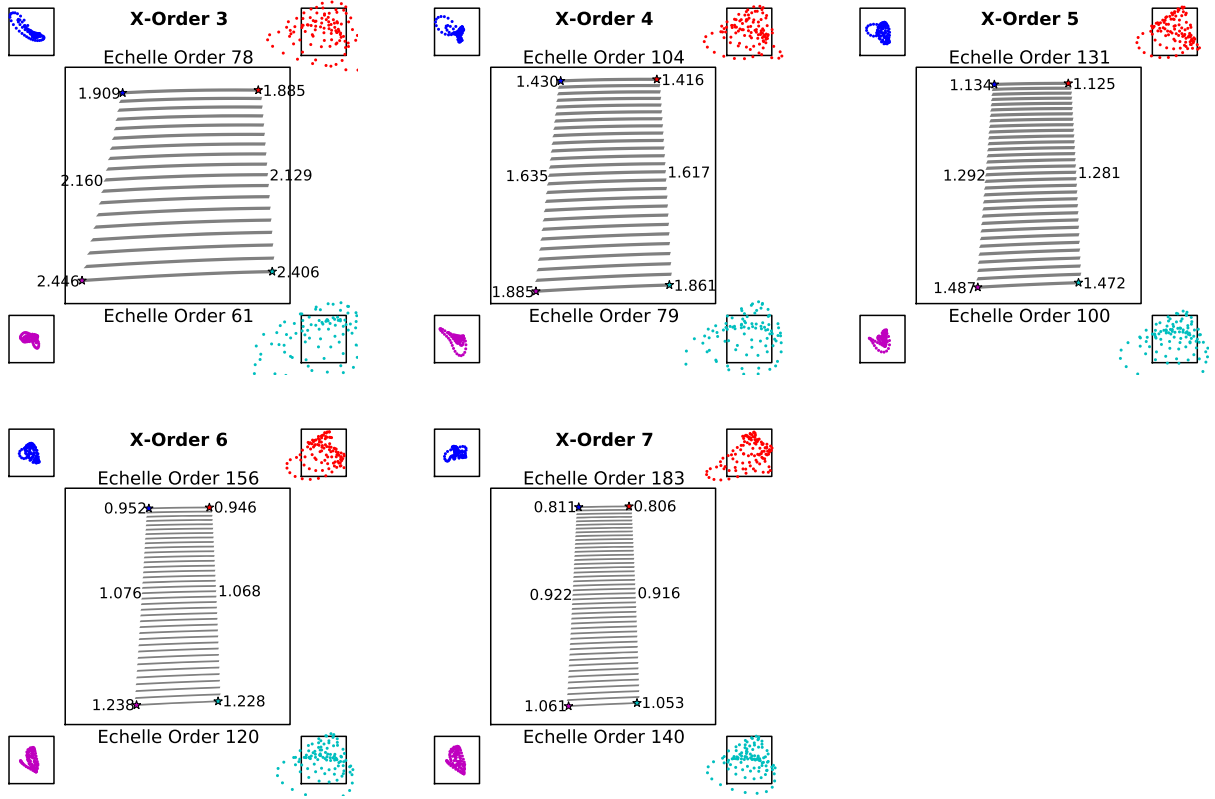


Figure 5. Ray-traced echellograms and corner spot diagrams for each observing mode of NEWS, selectable entirely by filter wheel. The filter selects an order of the cross-dispersing grating (orders 3 through 7), resulting in wavelength coverage from 0.8 to 2.5 μm . The large boxes represent the size of the full Hawaii-2RG detector (36.9 x 36.9 mm) and the small boxes represent the size of each pixel (18 x 18 μm). By using a Mangin reflector in combination with a conjugate paraboloid, aberrations introduced by the collimating paraboloid are reduced to roughly a pixel. The aberrations from the paraboloid dominate the RMS spot sizes so that the tolerances on the optical surfaces are large (typically 10 μm), except for the Offner relay (1 μm).

3.2 Optical Performance

We optimized the camera lenses and Mangin fold mirror to minimize the RMS spot size across the detector. The largest source of aberration is wavelength-dependent field curvature introduced by dispersing onto the paraboloid, much of which is removed by the Mangin mirror. As a result, tolerances on the optical surfaces are quite large ($\sim 10 \mu\text{m}$). In Figure 5, we show the full simulated echellogram and corner spot diagrams. RMS spot sizes are on the order of one 18 μm square pixel.

4. MECHANICAL DESIGN

4.1 Optomechanical design

Figure 6 shows the full NEWS optomechanical design.

4.1.1 Optical bench

To simplify mounting and maintain a compact design, we designed all the optical components of NEWS to lie in a single plane. The mounts for each optical component all attach directly to a monolithic optical bench milled from a single block of 6061-T6 aluminum. To minimize weight, but maintain rigidity, the optical bench is

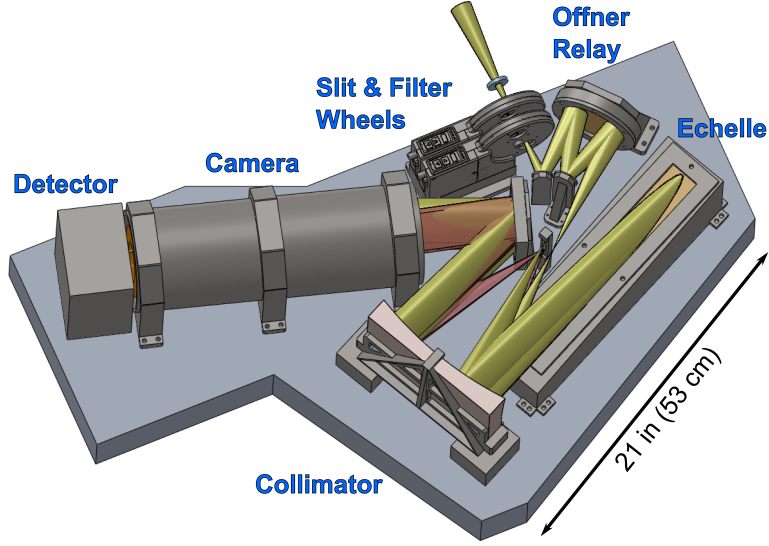


Figure 6. CAD rendering of the full NEWS optomechanical design. The optical bench and all mounts will be custom machined from 6061-T6 Al.

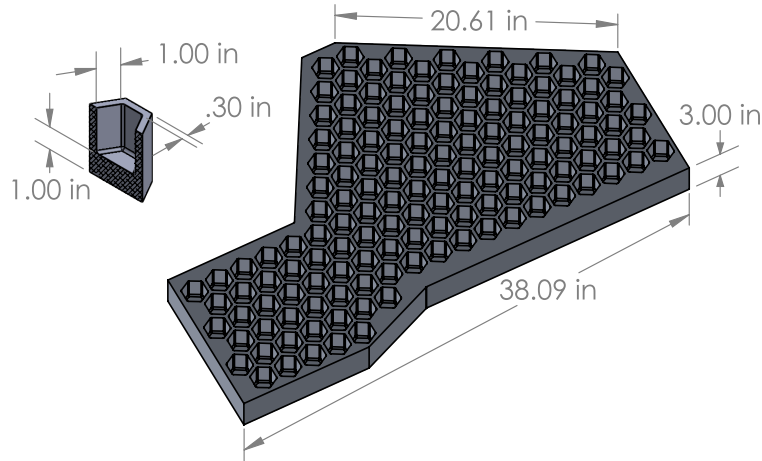


Figure 7. CAD rendering of the NEWS custom honeycomb optical bench (the bottom side as shown in Figure 6). An inset on the left shows a cross section of one of the honeycomb hexagons. The hexagons are 1 inch on a side (inner) with 0.3 inch thick walls and are milled 2 inches deep, leaving 1 inch of solid aluminum for the mounting surface.

light-weighted with a honeycomb structure. The hexagons of the honeycomb are milled 2 inches deep with 1 inch sides (inner), leaving 0.3 inch thick walls and 1 inch of solid aluminum for the mounting surface. Figure 7 shows the light-weighted honeycomb structure. The optical bench will be surrounded by a low-emissivity radiation shield and mounted to an enclosing cryostat via G10 tabs.

We applied finite element analysis (FEA) on the optical bench to ensure it meets mechanical tolerances ($< 10\mu\text{m}$ flex) under the weight of the optical elements subject to varied gravity vectors.

4.1.2 Optics Mounts

We designed all optical mounts to be machined out of 6061-T6 Al. To maintain optical positioning tolerances, we employ flexure supports on all optics to compensate for thermal contraction stress and to preload against a changing gravity vector. For example, the Offner relay primary mirror is constrained by a radial flexure ring with 16 EDM wire-cut spring restraints (see Figure 8). The design is identical to that used in NIHTS.⁵²

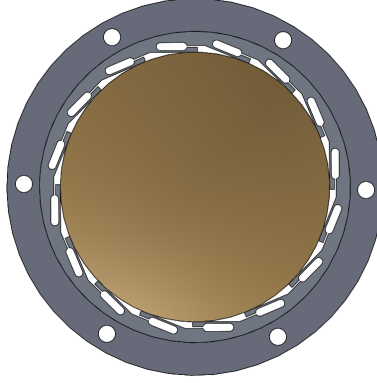


Figure 8. CAD rendering of radial flexure ring mount for the Offner relay primary mirror. Wire-cut spring restraints compensate for thermal contraction stress and preload against a changing gravity vector.

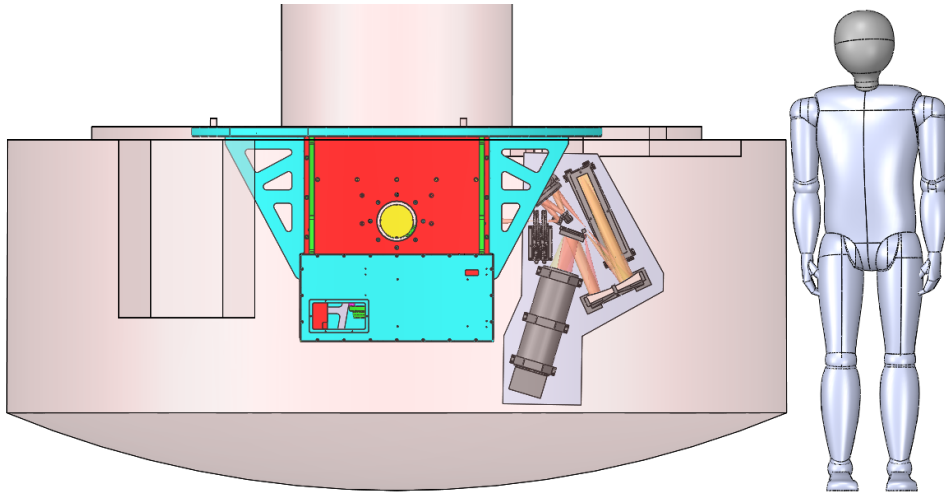


Figure 9. CAD rendering of the NEWS mechanical design as it would be positioned on the DCT instrument cube. A cryostat containing the instrument would be mounted directly to one of the large ports on the instrument cube. The interference-free volume for the instrument cube is shown in transparent red. NEWS fits within the size constraints of mounting to the DCT. A six-foot-tall human figure is shown for scale.

4.2 Mounting to the DCT

We designed NEWS within the size and weight restrictions of mounting to one of the large ports on the DCT's instrument cube at the Cassegrain focus of the telescope. The instrument cube rotates to maintain constant field alignment. Instruments mounted to the cube must clear the telescope mount supports at all rotation angles and the mount platform at all altitudes. Mounting directly to the telescope entails strict weight constraints. The total payload capability for the instrument cube is 1500 kg.⁵⁴ The large instrument ports each can support up to 360 kg.⁵¹ Our current design fits within a $99 \times 64 \times 30$ cm in volume and weighs less than 100 kg (excluding the cryostat).

4.2.1 Software System

Software control and interfacing to the TCS will be done with the Lowell Observatory LOIS⁵⁵/LOUI systems which handle the current instrument suit on the DCT. This software system is a mature well defined control system that already has interfaces to the TCS, Guider, and AOS subsystems. If we decide that the ARC controller is the best match for NEWS then most of the interfacing to the detector has already been done for the NIHTS instrument, an H2RG NIR instrument and Mimir, an Aladdin III instrument.

4.3 Thermal Management

Thermal modeling of NEWS shows that the predictive radiative load will be around 63 W at 300 K, assuming a polished aluminum cold shield wrapped in MLI and based on the current surface area of the instrument cold shield. Average high temperatures are 301 K for the hottest month of the year in Happy Jack, Arizona where DCT is located. This load can be easily handled by a CTI 1050 single stage cryodyne refrigeration unit which is capable of delivering 80 W of cooling at 78 K with enough overhead to handle any parasitic load from the wiring and the intermittent load of the motors. We will utilize thick copper strapping to the cold bench and shield with a much small copper line to the detector for the conductive paths for heat transfer. This line to the detector will have a small sapphire disk spacer to minimize the electrical noise transferred to the detector. We will monitor and control the instrument stability, cool down and warm up rates via a Lakeshore model 331 temperature controller.

5. SUMMARY

We have designed a high-resolution NIR spectrograph for the 4.3-meter Discovery Channel Telescope. NEWS achieves a resolution of $R = 60,000$ over the full 0.8–2.5 μm range. Our design offers continuous coverage within each of its five observing modes corresponding to the photometric z-, Y-, J-, H-, and K-bands. If built, NEWS will be uniquely capable of measuring the composition and ages of field M dwarfs, including those who host planets detected by *TESS*.

ACKNOWLEDGMENTS

Support for this work was provided by the Department of Astronomy and the Institute for Astrophysical Research at Boston University. This research made use of the Massachusetts Green High Performance Computing Center in Holyoke, MA.

REFERENCES

- [1] Muirhead, P. S., Hall, Z. J., and Veyette, M. J., “HiJaK: the high-resolution J, H and K spectrometer,” in [*Ground-based and Airborne Instrumentation for Astronomy V*], Proc. SPIE **9147**, 91477T (Aug. 2014).
- [2] McLean, I. S., Becklin, E. E., Bendiksen, O., Brims, G., Canfield, J., Figer, D. F., Graham, J. R., Hare, J., Lacayanga, F., Larkin, J. E., Larson, S. B., Levenson, N., Magnone, N., Teplitz, H., and Wong, W., “Design and development of NIRSPEC: a near-infrared echelle spectrograph for the Keck II telescope,” in [*Infrared Astronomical Instrumentation*], Fowler, A. M., ed., *Society of Photo-Optical Instrumentation Engineers (SPIE) Conference Series* **3354**, 566–578 (Aug. 1998).
- [3] Kaeuf, H.-U., Ballester, P., Biereichel, P., Delabre, B., Donaldson, R., Dorn, R., Fedrigo, E., Finger, G., Fischer, G., Franza, F., Gojak, D., Huster, G., Jung, Y., Lizon, J.-L., Mehrgan, L., Meyer, M., Moorwood, A., Pirard, J.-F., Paufigue, J., Pozna, E., Siebenmorgen, R., Silber, A., Stegmeier, J., and Wegerer, S., “CRIRES: a high-resolution infrared spectrograph for ESO’s VLT,” in [*Ground-based Instrumentation for Astronomy*], Moorwood, A. F. M. and Iye, M., eds., *Society of Photo-Optical Instrumentation Engineers (SPIE) Conference Series* **5492**, 1218–1227 (Sept. 2004).
- [4] Tokunaga, A. T., Kobayashi, N., Bell, J., Ching, G. K., Hodapp, K.-W., Hora, J. L., Neill, D., Onaka, P. M., Rayner, J. T., Robertson, L., Warren, D. W., Weber, M., and Young, T. T., “Infrared camera and spectrograph for the SUBARU Telescope,” in [*Infrared Astronomical Instrumentation*], Fowler, A. M., ed., Proc. SPIE **3354**, 512–524 (Aug. 1998).
- [5] Kobayashi, N., Tokunaga, A. T., Terada, H., Goto, M., Weber, M., Potter, R., Onaka, P. M., Ching, G. K., Young, T. T., Fletcher, K., Neil, D., Robertson, L., Cook, D., Imanishi, M., and Warren, D. W., “IRCS: infrared camera and spectrograph for the Subaru Telescope,” in [*Optical and IR Telescope Instrumentation and Detectors*], Iye, M. and Moorwood, A. F., eds., Proc. SPIE **4008**, 1056–1066 (Aug. 2000).
- [6] Levine, S. E., Bida, T. A., Chylek, T., Collins, P. L., DeGroot, W. T., Dunham, E. W., Lotz, P. J., Venetiu, A. J., and Zoonemat Kermani, S., “Status and performance of the Discovery Channel Telescope during commissioning,” in [*Society of Photo-Optical Instrumentation Engineers (SPIE) Conference Series*], *Society of Photo-Optical Instrumentation Engineers (SPIE) Conference Series* **8444** (Sept. 2012).

- [7] Yuk, I.-S., Jaffe, D. T., Barnes, S., Chun, M.-Y., Park, C., Lee, S., Lee, H., Wang, W., Park, K.-J., Pak, S., Strubhar, J., Deen, C., Oh, H., Seo, H., Pyo, T.-S., Park, W.-K., Lacy, J., Goertz, J., Rand, J., and Gully-Santiago, M., “Preliminary design of IGRINS (Immersion GRating INfrared Spectrograph),” in [*Society of Photo-Optical Instrumentation Engineers (SPIE) Conference Series*], *Society of Photo-Optical Instrumentation Engineers (SPIE) Conference Series* **7735** (July 2010).
- [8] Rayner, J., Bond, T., Bonnet, M., Jaffe, D., Muller, G., and Tokunaga, A., “iSHELL: a 1-5 micron cross-dispersed $R=70,000$ immersion grating spectrograph for IRTF,” in [*Society of Photo-Optical Instrumentation Engineers (SPIE) Conference Series*], *Society of Photo-Optical Instrumentation Engineers (SPIE) Conference Series* **8446** (Sept. 2012).
- [9] Bochanski, J. J., Hawley, S. L., Covey, K. R., West, A. A., Reid, I. N., Golimowski, D. A., and Ivezić, Ž., “The Luminosity and Mass Functions of Low-mass Stars in the Galactic Disk. II. The Field,” *AJ* **139**, 2679–2699 (June 2010).
- [10] Morton, T. D. and Swift, J., “The Radius Distribution of Planets around Cool Stars,” *ApJ* **791**, 10 (Aug. 2014).
- [11] Dressing, C. D. and Charbonneau, D., “The Occurrence of Potentially Habitable Planets Orbiting M Dwarfs Estimated from the Full Kepler Dataset and an Empirical Measurement of the Detection Sensitivity,” *ApJ* **807**, 45 (July 2015).
- [12] Sullivan, P. W., Winn, J. N., Berta-Thompson, Z. K., Charbonneau, D., Deming, D., Dressing, C. D., Latham, D. W., Levine, A. M., McCullough, P. R., Morton, T., Ricker, G. R., Vanderspek, R., and Woods, D., “The Transiting Exoplanet Survey Satellite: Simulations of Planet Detections and Astrophysical False Positives,” *ApJ* **809**, 77 (Aug. 2015).
- [13] Charbonneau, D., Berta, Z. K., Irwin, J., Burke, C. J., Nutzman, P., Buchhave, L. A., Lovis, C., Bonfils, X., Latham, D. W., Udry, S., Murray-Clay, R. A., Holman, M. J., Falco, E. E., Winn, J. N., Queloz, D., Pepe, F., Mayor, M., Delfosse, X., and Forveille, T., “A super-Earth transiting a nearby low-mass star,” *Nature* **462**, 891–894 (Dec. 2009).
- [14] Muirhead, P. S., Johnson, J. A., Apps, K., Carter, J. A., Morton, T. D., Fabrycky, D. C., Pineda, J. S., Bottom, M., Rojas-Ayala, B., Schlawin, E., Hamren, K., Covey, K. R., Crepp, J. R., Stassun, K. G., Pepper, J., Hebb, L., Kirby, E. N., Howard, A. W., Isaacson, H. T., Marcy, G. W., Levitan, D., Diaz-Santos, T., Armus, L., and Lloyd, J. P., “Characterizing the Cool KOIs. III. KOI 961: A Small Star with Large Proper Motion and Three Small Planets,” *ApJ* **747**, 144 (Mar. 2012).
- [15] Muirhead, P. S., Mann, A. W., Vanderburg, A., Morton, T. D., Kraus, A., Ireland, M., Swift, J. J., Feiden, G. A., Gaidos, E., and Gazak, J. Z., “Kepler-445, Kepler-446 and the Occurrence of Compact Multiples Orbiting Mid-M Dwarf Stars,” *ApJ* **801**, 18 (Mar. 2015).
- [16] Dressing, C. D. and Charbonneau, D., “The Occurrence Rate of Small Planets around Small Stars,” *ApJ* **767**, 95 (Apr. 2013).
- [17] Lopez, E. D., *Understanding Kepler’s super-Earths and sub-Neptunes: Insights from thermal evolution and photo-evaporation*, PhD thesis, University of California, Santa Cruz (2014).
- [18] Wu, Y. and Goldreich, P., “Tidal Evolution of the Planetary System around HD 83443,” *ApJ* **564**, 1024–1027 (Jan. 2002).
- [19] Jackson, B., Greenberg, R., and Barnes, R., “Tidal Evolution of Close-in Extrasolar Planets,” *ApJ* **678**, 1396–1406 (May 2008).
- [20] Morgan, D. P., West, A. A., Garcés, A., Catalán, S., Dhital, S., Fuchs, M., and Silvestri, N. M., “The Effects of Close Companions (and Rotation) on the Magnetic Activity of M Dwarfs,” *AJ* **144**, 93 (Oct. 2012).
- [21] West, A. A., Weisenburger, K. L., Irwin, J., Berta-Thompson, Z. K., Charbonneau, D., Dittmann, J., and Pineda, J. S., “An Activity-Rotation Relationship and Kinematic Analysis of Nearby Mid-to-Late-Type M Dwarfs,” *ApJ* **812**, 3 (Oct. 2015).
- [22] Newton, E. R., Irwin, J., Charbonneau, D., Berta-Thompson, Z. K., Dittmann, J. A., and West, A. A., “The Rotation and Galactic Kinematics of Mid M Dwarfs in the Solar Neighborhood,” *ApJ* **821**, 93 (Apr. 2016).
- [23] Feuillet, D. K., Bovy, J., Holtzman, J., Girardi, L., MacDonald, N., Majewski, S. R., and Nidever, D. L., “Determining Ages of APOGEE Giants with Known Distances,” *ApJ* **817**, 40 (Jan. 2016).

- [24] Haywood, M., Di Matteo, P., Lehnert, M. D., Katz, D., and Gómez, A., “The age structure of stellar populations in the solar vicinity. Clues of a two-phase formation history of the Milky Way disk,” *A&A* **560**, A109 (Dec. 2013).
- [25] Bensby, T., Feltzing, S., and Oey, M. S., “Exploring the Milky Way stellar disk. A detailed elemental abundance study of 714 F and G dwarf stars in the solar neighbourhood,” *A&A* **562**, A71 (Feb. 2014).
- [26] Martig, M., Rix, H.-W., Aguirre, V. S., Hekker, S., Mosser, B., Elsworth, Y., Bovy, J., Stello, D., Anders, F., García, R. A., Tayar, J., Rodrigues, T. S., Basu, S., Carrera, R., Ceillier, T., Chaplin, W. J., Chiappini, C., Frinchaboy, P. M., García-Hernández, D. A., Hearty, F. R., Holtzman, J., Johnson, J. A., Majewski, S. R., Mathur, S., Mészáros, S., Miglio, A., Nidever, D., Pan, K., Pinsonneault, M., Schiavon, R. P., Schneider, D. P., Serenelli, A., Shetrone, M., and Zamora, O., “Young α -enriched giant stars in the solar neighbourhood,” *MNRAS* **451**, 2230–2243 (Aug. 2015).
- [27] Önehag, A., Heiter, U., Gustafsson, B., Piskunov, N., Plez, B., and Reiners, A., “M-dwarf metallicities. A high-resolution spectroscopic study in the near infrared,” *A&A* **542**, A33 (June 2012).
- [28] Lindgren, S., Heiter, U., and Seifahrt, A., “Metallicity determination of M dwarfs. High-resolution infrared spectroscopy,” *A&A* **586**, A100 (Feb. 2016).
- [29] Pineda, J. S., Bottom, M., and Johnson, J. A., “Using High-resolution Optical Spectra to Measure Intrinsic Properties of Low-mass Stars: New Properties for KOI-314 and GJ 3470,” *ApJ* **767**, 28 (Apr. 2013).
- [30] Neves, V., Bonfils, X., Santos, N. C., Delfosse, X., Forveille, T., Allard, F., and Udry, S., “Metallicity of M dwarfs. IV. A high-precision $[\text{Fe}/\text{H}]$ and T_{eff} technique from high-resolution optical spectra for M dwarfs,” *A&A* **568**, A121 (Aug. 2014).
- [31] Maldonado, J., Affer, L., Micela, G., Scandariato, G., Damasso, M., Stelzer, B., Barbieri, M., Bedin, L. R., Biazzo, K., Bignamini, A., Borsa, F., Claudi, R. U., Covino, E., Desidera, S., Esposito, M., Gratton, R., González Hernández, J. I., Lanza, A. F., Maggio, A., Molinari, E., Pagano, I., Perger, M., Pillitteri, I., Piotto, G., Poretti, E., Prisinzano, L., Rebolo, R., Ribas, I., Shkolnik, E., Southworth, J., Sozzetti, A., and Suárez Mascareño, A., “Stellar parameters of early-M dwarfs from ratios of spectral features at optical wavelengths,” *A&A* **577**, A132 (May 2015).
- [32] Rojas-Ayala, B., Covey, K. R., Muirhead, P. S., and Lloyd, J. P., “Metal-rich M-Dwarf Planet Hosts: Metallicities with K-band Spectra,” *ApJ* **720**, L113–L118 (Sept. 2010).
- [33] Rojas-Ayala, B., Covey, K. R., Muirhead, P. S., and Lloyd, J. P., “Metallicity and Temperature Indicators in M Dwarf K-band Spectra: Testing New and Updated Calibrations with Observations of 133 Solar Neighborhood M Dwarfs,” *ApJ* **748**, 93 (Apr. 2012).
- [34] Terrien, R. C., Mahadevan, S., Bender, C. F., Deshpande, R., Ramsey, L. W., and Bochanski, J. J., “An H-band Spectroscopic Metallicity Calibration for M Dwarfs,” *ApJ* **747**, L38 (Mar. 2012).
- [35] Mann, A. W., Brewer, J. M., Gaidos, E., Lépine, S., and Hilton, E. J., “Prospecting in Late-type Dwarfs: A Calibration of Infrared and Visible Spectroscopic Metallicities of Late K and M Dwarfs Spanning 1.5 dex,” *AJ* **145**, 52 (Feb. 2013).
- [36] Newton, E. R., Charbonneau, D., Irwin, J., Berta-Thompson, Z. K., Rojas-Ayala, B., Covey, K., and Lloyd, J. P., “Near-infrared Metallicities, Radial Velocities, and Spectral Types for 447 Nearby M Dwarfs,” *AJ* **147**, 20 (Jan. 2014).
- [37] Bonfils, X., Delfosse, X., Udry, S., Santos, N. C., Forveille, T., and Ségransan, D., “Metallicity of M dwarfs. I. A photometric calibration and the impact on the mass-luminosity relation at the bottom of the main sequence,” *A&A* **442**, 635–642 (Nov. 2005).
- [38] Casagrande, L., Flynn, C., and Bessell, M., “M dwarfs: effective temperatures, radii and metallicities,” *MNRAS* **389**, 585–607 (Sept. 2008).
- [39] Johnson, J. A. and Apps, K., “On the Metal Richness of M Dwarfs with Planets,” *ApJ* **699**, 933–937 (July 2009).
- [40] Schlafman, K. C. and Laughlin, G., “A physically-motivated photometric calibration of M dwarf metallicity,” *A&A* **519**, A105+ (Sept. 2010).
- [41] Neves, V., Bonfils, X., Santos, N. C., Delfosse, X., Forveille, T., Allard, F., Natário, C., Fernandes, C. S., and Udry, S., “Metallicity of M dwarfs. II. A comparative study of photometric metallicity scales,” *A&A* **538**, A25 (Feb. 2012).

- [42] Johnson, J. A., Gazak, J. Z., Apps, K., Muirhead, P. S., Crepp, J. R., Crossfield, I. J. M., Boyajian, T., von Braun, K., Rojas-Ayala, B., Howard, A. W., Covey, K. R., Schlawin, E., Hamren, K., Morton, T. D., Marcy, G. W., and Lloyd, J. P., “Characterizing the Cool KOIs. II. The M Dwarf KOI-254 and Its Hot Jupiter,” *AJ* **143**, 111 (May 2012).
- [43] Hejazi, N., De Robertis, M. M., and Dawson, P. C., “Optical-Near Infrared Photometric Calibration of M Dwarf Metallicity and Its Application,” *AJ* **149**, 140 (Apr. 2015).
- [44] Veyette, M. J., Muirhead, P. S., Mann, A. W., and Allard, F., “The Physical Mechanism Behind M Dwarf Metallicity Indicators and the Role of C and O Abundances,” *ApJ* **828**, 95 (Sept. 2016).
- [45] Tsuji, T. and Nakajima, T., “Near-infrared spectroscopy of M dwarfs. I. CO molecule as an abundance indicator of carbon,” *PASJ* **66**, 98 (Oct. 2014).
- [46] Tsuji, T., Nakajima, T., and Takeda, Y., “Near-infrared spectroscopy of M dwarfs. II. H₂O molecule as an abundance indicator of oxygen,” *PASJ* **67**, 26 (Apr. 2015).
- [47] Tsuji, T. and Nakajima, T., “Near-infrared spectroscopy of M dwarfs. III. Carbon and oxygen abundances in late M dwarfs, including the dusty rapid rotator 2MASS J1835379+325954,” *PASJ* **68**, 13 (Feb. 2016).
- [48] Origlia, L., Oliva, E., Baffa, C., Falcini, G., Giani, E., Massi, F., Montegriffo, P., Sanna, N., Scuderi, S., Sozzi, M., Tozzi, A., Carleo, I., Gratton, R., Ghinassi, F., and Lodi, M., “High resolution near IR spectroscopy with GIANO-TNG,” in [*Ground-based and Airborne Instrumentation for Astronomy V*], Proc. SPIE **9147**, 91471E (July 2014).
- [49] Herter, T. L., Henderson, C. P., Wilson, J. C., Matthews, K. Y., Rahmer, G., Bonati, M., Muirhead, P. S., Adams, J. D., Lloyd, J. P., Skrutskie, M. F., Moon, D., Parshley, S. C., Nelson, M. J., Martinache, F., and Gull, G. E., “The performance of TripleSpec at Palomar,” in [*Society of Photo-Optical Instrumentation Engineers (SPIE) Conference Series*], *Society of Photo-Optical Instrumentation Engineers (SPIE) Conference Series* **7014** (Aug. 2008).
- [50] Elias, J. H., Vukobratovich, D., Andrew, J. R., Cho, M. K., Cuberly, R. W., Don, K., Gerzoff, A., Harmer, C. F., Harris, D., Heynssens, J. B., Hicks, J., Kovacs, A., Li, C., Liang, M., Moon, I. K., Pearson, E. T., Plum, G., Roddier, N. A., Tvedt, J., Wolff, R. J., and Wong, W.-Y., “Design of the Gemini near-infrared spectrometer,” in [*Infrared Astronomical Instrumentation*], Fowler, A. M., ed., Proc. SPIE **3354**, 555–565 (Aug. 1998).
- [51] Bida, T. A., Dunham, E. W., Nye, R. A., Chylek, T., and Oliver, R. C., “Design, development, and testing of the DCT Cassegrain instrument support assembly,” in [*Society of Photo-Optical Instrumentation Engineers (SPIE) Conference Series*], *Society of Photo-Optical Instrumentation Engineers (SPIE) Conference Series* **8444** (Sept. 2012).
- [52] Bida, T. A., Dunham, E. W., Massey, P., and Roe, H. G., “First-generation instrumentation for the Discovery Channel Telescope,” in [*Ground-based and Airborne Instrumentation for Astronomy V*], Proc. SPIE **9147**, 91472N (July 2014).
- [53] Clemens, D. P., Sarcia, D., Grabau, A., Tollestrup, E. V., Buie, M. W., Dunham, E., and Taylor, B., “Mimir: A Near-Infrared Wide-Field Imager, Spectrometer and Polarimeter,” *PASP* **119**, 1385–1402 (Dec. 2007).
- [54] Smith, B., Chylek, T., Degroff, B., Finley, D., Hall, J., Lotz, P. J., McCreight, B., and Venetiou, A., “The Discovery Channel Telescope: early integration,” in [*Society of Photo-Optical Instrumentation Engineers (SPIE) Conference Series*], *Society of Photo-Optical Instrumentation Engineers (SPIE) Conference Series* **7733** (July 2010).
- [55] Taylor, B. W., Dunham, E. W., Gould, A. J., Osip, D. J., and Elliot, J. L., “Lowell Observatory instrumentation system (LOIS): a modular control system for astronomical instrumentation,” in [*Advanced Telescope and Instrumentation Control Software*], Lewis, H., ed., Proc. SPIE **4009**, 449–456 (June 2000).